DSS 43 Antenna Gain Analysis for Voyager Uranus Encounter: 8.45-GHz Radio Science Data Correction

S. D. Slobin and W. A. Imbriale
Radio Frequency and Microwave Subsystems Section

A malfunction of the DSN 64-meter antenna in Australia forced the antenna to operate with a mispositioned subreflector during the Voyager Uranus encounter period (January 24, 1986). Because of changing main reflector shape and quadripod position as a function of elevation angle, the antenna gain and pointing were not as expected, and the 8.45-GHz received signal level changed during the pass. The study described here used Geometrical Theory of Diffraction (GTD) analysis to determine actual antenna gain and pointing during that period in an attempt to reconstruct the radio science data. It is found that 1.4 dB of signal variation can be accounted for by antenna geometry changes and pointing error. Suggested modifications to the values measured during the pass are presented. Additionally, an extremely useful tool for the analysis of gravity-deformed reflectors was developed for use in future antenna design and analysis projects.

I. Introduction

A series of DSS 43 64-m antenna system failures during the Voyager Uranus encounter on January 24, 1986, affected the quality of radio science data taken during the occultation phase of the encounter. In particular, an antenna elevation angle encoder failed and was removed from service (disconnected). This failure, in turn, caused the subreflector controller (SRC) to command the subreflector to move as though it were operating in its normal gain-peaking mode, although at a much faster rate. After about 12 minutes, the subreflector movement was automatically stopped because of a previously planned decision to turn off the SRC. The antenna continued to track the spacecraft for the rest of the pass, but the antenna had a mispositioned subreflector, which affected both antenna gain and pointing. All calculations described here were carried out for a frequency of 8.45 GHz.

This article presents the results of a study undertaken to analyze antenna performance using JPL-developed GTD (geometrical theory of diffraction) computer programs and other programs[1] to determine antenna shape as a function of gravity loading at different elevation angles. These programs define the geometry of the problem, taking into consideration quadripod sag and subreflector position, in order to determine antenna gain and pointing with respect to spacecraft location.

It was planned that during the encounter sequence, the gain-peaking would be turned off, because the subreflector motion required to make the correction would introduce unwanted

[1] T. Veruttipong, D. Rochblatt, W. Imbriale, V. Galindo, *Dual Shaped and Conic GTD/Jacobi-Bessel Analysis Programs, A User Manual*, JPL D-2538 (internal document), Jet Propulsion Laboratory, Pasadena, Calif.

phase error in the received signal. It was determined that normal tracking would continue until the antenna reached an elevation angle of 64 degrees. Previous to this time, both y (vertical) and z (axial) subreflector movements were made to continuously peak the gain during the track. In addition, antenna pointing correction (squint correction) was made to reposition the beam on the spacecraft, since the y–z subreflector motion moved the beam continuously. Above 64 degrees elevation, the subreflector would remain fixed and pointing would be optimized by previous conscan use (discontinued a half-hour earlier). It was expected that the gain loss due to the lack of subreflector focusing would be acceptable.

The resultant condition of the antenna in its "failed" mode was this: (1) An initial step-function pointing error occurred due to the subreflector movement, not entirely compensated for by squint correction; (2) the pointing error changed throughout the pass as the antenna elevation approached or departed from the elevation angle corresponding to the failed subreflector position; (3) an initial step-function gain loss occurred because of a misfocused subreflector; and (4) this gain loss changed as the antenna elevation approached or departed from the elevation angle corresponding to the failed subreflector position.

II. Physical Description of Antenna Deformations

The gravity loading on large antennas causes quite large (up to 1 inch) deformations of surface shape, and causes movements of the quadripod structure that misposition the subreflector. The accepted coordinate system description for an azimuth-elevation antenna is that with the antenna pointing at the southern horizon, and an observer looking into the face of the dish, the $+y$ direction is at the top of the dish, $+x$ is toward the east/right edge of the dish, and the $+z$ axis comes out from the center of the dish toward the observer. Typically, the origin of this coordinate system is the center of the dish surface. This is not a requirement, however, as the dish shape can be defined in any coordinate system.

At a 45-degree elevation angle, the DSS 43 64-m antenna structure is designed and set to be "perfect," i.e., the main reflector is a perfect paraboloid, and the quadripod structure is located so that with the subreflector at some reference point, its virtual focus (on the concave side of the hyperboloidal subreflector) is coincident with the focus of the paraboloid. Thus, antenna gain is maximized and the resultant antenna beam is located precisely on the $+z$ axis. The DSN 64-m antennas have been designed to take into account structural deformations so that antenna pointing is maintained under gravity loading at elevation angles differing from 45 degrees [1]. In other words, when the antenna elevatio changes from 45 to 60 degrees, the beam moves up to 6 degrees, not 59.9 degrees. Unfortunately, this design result in a slightly degraded antenna gain. To overcome the gai loss, the subreflector is repositioned in z and y axes to plac its focus coincident with the best-fit focus of the distorte main reflector. The resulting pointing error is taken out b means of antenna movement known as "squint correction."

At angles higher than 45 degrees, the main reflector dis flattens out, its focal length increases, and the quadripod sag in both the $+y$ and $-z$ directions. The $-z$ movement ca probably be explained by the base of the quadripod legs bein pulled downward by the sagging backup structure. The dis tortions in the main reflector alone cause the beam to swin upward in the $+y$ direction. The sagging quadripod (also in th $+y$ direction) moves the subreflector, and this motion move the beam back down toward the $-y$ direction. These effect nearly cancel out (to better than 0.010 degrees over th 35- to 75-degree elevation range). To recapture gain, th subreflector is moved (for this example) in the $+z$ and $-$ directions. The resultant beam moves in the $+y$ direction, an this requires a downward (negative) squint correction. A 80-degree elevation angle, the subreflector movements fo z and y are, respectively, 0.34 and –2.57 inches. The squin correction is –0.0938 degrees. For comparison, the 3-dB beam width of a 64-m antenna operating at X-band is approximatel 0.036 degrees.

For antenna elevations of less than 45 degrees, the top edg falls forward, the dish deepens, the focal length is reduced, an the quadripod falls downward toward the ground and ou ward away from the main reflector. The dish movemen pushes the beam down, and the quadripod movement brings i back. The required subreflector movement to peak the gain i inward ($-z$) and up ($+y$). At 10-degree elevation, the z and movements are –0.57 and +1.34 inches, and the squint correc tion is +0.0488 degrees.

III. Computational Methods

All calculations used in this study began with a descriptio of the main reflector. The x, y, and z coordinates of 275 poin on one-half the dish surface (the $+x$ half-plane) were obtaine from the JPL Ground Antenna Engineering Section.[2] Th other half of the dish was developed, and the x, y, and z coo dinates of the dish under gravity loading were calculated elevation angles of interest using structural deformation valu also obtained from that Section. The GTD technique requir

[2]R. Levy and M. S. Katow, Ground Antenna and Facilities Engineeri Section, Jet Propulsion Laboratory, Pasadena, Calif., personal co munication, July 1986.

what is known as a "global" description of the main reflector surface using Jacobi-Fourier polynomials [2]. The resulting coefficients are used in the GTD program itself in order to calculate the field scattered by the main reflector. In this analysis, it is assumed that the subreflector is hyperboloidal in shape and does not change shape due to gravity loading.

The GTD program uses a geometrical theory of diffraction analysis to compute the scattered near fields from the subreflector and a physical optics analysis (Jacobi-Bessel algorithm) to compute the scattered far fields from the main reflector using the subreflector fields as input. The program can handle arbitrarily shaped surfaces for both the subreflector and main reflector with respect to the main reflector system. A complete description of the program is given elsewhere.[3]

Inputs to the GTD program include geometric descriptions of the feed system. In particular, the feedhorn (dual-mode hybrid horn) is located in the upper left feedcone (of three) as seen looking into the dish. The subreflector coordinate system is located at the phase center of the feedhorn at a 45-degree antenna elevation angle. Under sagged conditions, the subreflector coordinate system and feedhorn are considered to move with the quadripod structure. This movement must be given as input, along with Euler angle rotation of the subreflector coordinate system itself in the main reflector coordinate system. Under sagged conditions, the feedhorn must be moved in the subreflector coordinate system to locate it back in the feedcone (assumed not to move as a function of elevation angle change and gravity loading). An Euler angle rotation of the feedhorn is necessary to adjust the polarization of the far-field pattern.

Thus, with the global surface description of the main reflector, and geometric inputs of subreflector and feedhorn position, the far-field Jacobi-Bessel coefficients can be calculated and the far-field gain and pointing for the antenna can be determined. By defining a center of expansion for the far-field coefficients, computational time may be reduced if one can quickly locate the antenna beam and examine its structure with fine resolution of the far-field coordinates.

IV. Results

The results of this study are given in the set of curves presented here. These curves show DSS 43 antenna performance during the Voyager Uranus occultation period (1986 024/2100 to 025/0300 GMT).

Figure 1 shows antenna elevation angle during the pass. Meridian transit is at 23:07:41 GMT at an elevation angle of 77.78 degrees. The actual spacecraft occultation occurred between about 23:20 and 00:40 GMT.

Figure 2 shows what the gain during normal operation of the antenna would have been with proper subreflector y and z focusing and perfect antenna pointing. The gains shown in these figures include only losses due to aperture illumination, feed and subreflector spillover, phase error, and cross-polarization. Other loss sources from small-scale surface roughness (Ruze loss), quadripod blockage, dissipative loss, and VSWR are not included. These losses are constant as a function of elevation angle and do not affect the results of the study presented here. Actual gain is approximately 2-dB less than shown in the figure. All curves of antenna gain show the inherent quality of the antenna as a function of main reflector shape and subreflector position only. They may be interpreted as the operational gain of the antenna when the beam is pointed perfectly at a spacecraft. Note that antenna gain is maximum at an elevation angle (Fig. 1) of 45 degrees.

Figure 3 is a combination of Figs. 1 and 2 and again shows a peak gain at an elevation angle of 45 degrees. Again, this is antenna performance with subreflector y–z focusing to peak up the gain. Because of computational resolution, the gain appears to be maximum over the range 45 to 50 degrees.

Figure 4 shows the position of the antenna beam relative to the main reflector z axis in the y–z plane. Note that y–z focusing to peak the gain causes relatively large movement of the beam. When the antenna is moved above 45-degree elevation, the beam ends up high. The opposite occurs below 45-degree elevation. The squint correction tables, which command antenna pointing to compensate for this beam movement, take their inputs from subreflector y and z position, and not from antenna elevation angle. In other words, the squint correction is not made as a function of elevation angle, but from subreflector position. In the DSS 43 problem being investigated here, the rapid subreflector movement over a 12-minute period caused a large and rapidly changing squint correction, even though the actual antenna elevation change was only 2 degrees. The beam movement predicted from GTD calculations differed slightly from that which was actually made using the squint correction tables. This is the source of the pointing error, resulting in a loss of received signal level (or equivalently, operational gain). The details of the squint correction error will be discussed later.

Figures 5–7 duplicate Figs. 2–4, differing only in the fact the GTD calculations were carried out with the subreflector fixed in a position corresponding to an elevation angle of 64 degrees. This is the position of the subreflector during a Voyager track 2 weeks before encounter, and was considered to be the "baseline reference signal level" with which actual encounter data would be compared.

[3]T. Veruttipong, et al., *op. cit.*

Figure 6 shows the gain versus elevation angle for the subreflector fixed at a position corresponding to the 64-degree elevation angle. Note the significant gain change, which is normally corrected with subreflector y–z focusing.

Figure 7 shows pointing versus elevation angle for the case with the subreflector fixed at 64-degree elevation. Note how pointing is maintained nearly constant when compared to the y–z focused case shown in Fig. 4.

Figures 8–10 are similar to Figs. 5–7, differing only in the fact that the subreflector is now in its failed position corresponding to an antenna elevation angle of 34 degrees. Figure 8 (gain versus time) shows the large loss experienced at meridian transit when the antenna elevation angle was 77.78 degrees.

Figure 9 shows gain versus elevation with the subreflector fixed at its 34-degree position.

Figure 10 shows antenna beam movement with elevation angle for a subreflector fixed at its 34-degree position. Note that the slope of this curve is the same as in Fig. 7. The beam position difference between the two curves is 0.063 degrees (approximately), almost two beamwidths of a 64-m antenna. This is the amount of beam movement that would be experienced during the uncontrolled subreflector movement if the antenna squint correction had been inoperative.

Figure 11 shows Figs. 2, 5, and 8 plotted on the same scale. Note that antenna gain with the subreflector fixed at the 64-degree position would have given performance nearly equal to the y–z focused subreflector for most of the pass. Only near the end of the pass, when the antenna was pointed at the lower elevation angles, would performance have been worse. The 34-degree subreflector case shows markedly degraded performance, except at the end of the pass, when its position was more nearly optimum for the low elevation antenna. All curves assume perfect antenna pointing and indicate the inherent gain of the antenna without regard to the spacecraft.

Figure 12 shows the gain advantage of y–z subreflector focusing compared to fixing the subreflector at a position corresponding to an antenna elevation of 64 degrees.

Figure 13 shows the gain advantage of y–z subreflector focusing compared to fixing the subreflector at a position corresponding to an antenna elevation of 34 degrees.

Figure 14 shows the gain loss (assuming perfect pointing) that would have been experienced under actual encounter conditions compared to performance measured 2 weeks previously with the subreflector fixed at 64 degrees. This curve is the difference between the 64-degree and 34-degree curves in Fig. 11. Because there is an additional loss due to pointing errors, this curve is not sufficient to adjust the Uranus encounter radio science data.

Figure 15 shows the pointing error resulting from incorrect squint correction. Before the encounter sequence period, up until 20:35 GMT, the spacecraft was tracked using conscan. This ensured virtually perfect pointing and maximum gain with the subreflector y–z focusing in operation. After conscan was turned off, 35 minutes elapsed before the elevation encoder failed and uncontrolled subreflector movement began. It is assumed that pointing remained perfect for this time period. During the subreflector movement period (21:09:54 to 21:22:07 GMT), the SRC was still operational, and the antenna squint correction very nearly kept up with the changing antenna beam position derived by the GTD analysis. At 21:22:07 GMT, the damage had been completed. For purposes of this analysis it is assumed that a step-function beam position error occurred. It was determined that the actual beam movement as derived by GTD was 0.0589 degrees. The antenna squint correction (which responded to the moving subreflector) corrected for 0.0625 degrees, leaving a step-function pointing error of 0.0036 degrees at 21:22:07 GMT, the time of SRC shutoff. In the figure, pointing error from 21:09 to 21:22 should be considered unreliable. Before 21:09, the pointing should be considered perfect. At 03:00 GMT, conscan was again turned on and it was found that the pointing residuals were approximately 0.001 degrees. For the purposes of this study, it was assumed that perfect pointing was achieved at this time.

Figure 16 shows the signal loss expected from bad pointing (incorrect squint correction) only. The values are calculated using a method presented in the DSN/Flight Project Interface Design Document.[4]

Figure 17 shows the final result of this study. The curve shows the actual signal loss during encounter compared to the track 2 weeks previous (with the subreflector at its fixed 64-degree elevation position). It is assumed that perfect pointing, using conscan or otherwise, was achieved during the previous track. This curve contains all items affecting loss of spacecraft signal, including antenna main reflector distortion, subreflector mispositioning, and gain loss due to errors in

[4] *Deep Space Network/Flight Project Interface Design Document* 810-5, Rev. D, TCI-10, Rec. C (internal document), Jet Propulsion Laboratory, Pasadena, Calif., 1977 and 1983.

squint correction. The losses presented in this curve are calculated from those in Fig. 14, added to those given in Fig. 16. It is suggested that this curve be used to upwardly modify measured values during the actual encounter sequence by the losses given in this curve. The resulting curve should be compared to the values measured during the 2-week earlier Voyager pass. Any differences in the two should be attributed to planetary ring structure, planetary atmosphere, or other phenomena.

Another adjustment to the radio science data should be made to account for the attenuating effect of the earth's atmosphere. This problem has not been addressed in this study. A nominal 8.5-GHz clear-air attenuation of 0.04 dB per airmass could be used if real-time estimates of the effect are unavailable.

V. Conclusion

The study presented here shows the efficacy of using GTD analysis to sort out the effects of rather complex antenna geometrical conditions due to gravitationally deformed main reflector surface and nonoptimum subreflector position. Both inherent gain degradation and signal loss due to pointing error can be determined for a variety of situations, planned and unplanned. The analysis technique was applied to the problem arising from an incorrectly positioned subreflector during the Voyager Uranus encounter of January 1986. The study concludes that 1.4 dB of received signal level variation can be accounted for, 1.15 dB from antenna deformation and subreflector misfocusing, and 0.25 dB due to pointing error loss. These results can be applied to the Voyager radio science data to eliminate the antenna-dependent loss of the received signal data.

Acknowledgment

The authors wish to thank the following persons for their assistance in this study. R. Levy and M. S. Katow of the Ground Antenna Engineering Section provided the main reflector surface description for the DSS 43 antenna under the effect of gravity loading. A. G. Cha and T. Veruttipong provided much needed aid in sorting out the intricacies of the GTD software. E. M. Andres was invaluable in providing computational assistance using the JPL Univac computer.

References

[1] M. S. Katow and M. Mori, *Computation of RF Boresight Direction From Reflector Distortions*, JPL Technical Report 32-1526, vol. XVII, pp. 78–82, Jet Propulsion Laboratory, Pasadena, Calif., 1973.

[2] V. Galindo-Israel, et al., "Interpolation methods for GTD analysis of shaped reflectors, *TDA Progress Report 42-80*, October–December 1984, pp. 62–67, Jet Propulsion Laboratory, Pasadena, Calif., February 15, 1985.

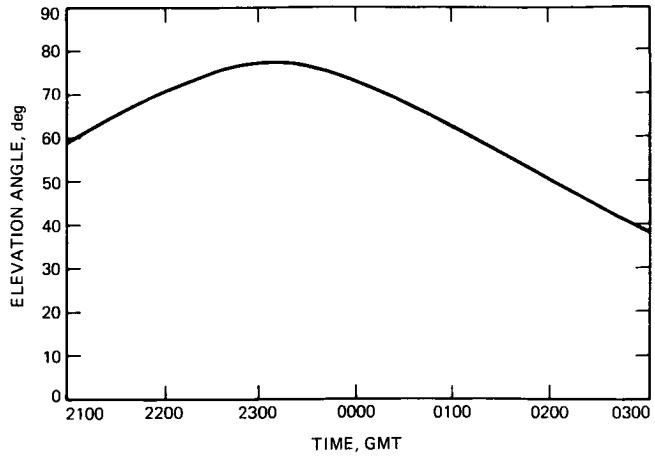

Fig. 1. DSS 43 antenna elevation angle vs time during Voyager Uranus encounter period

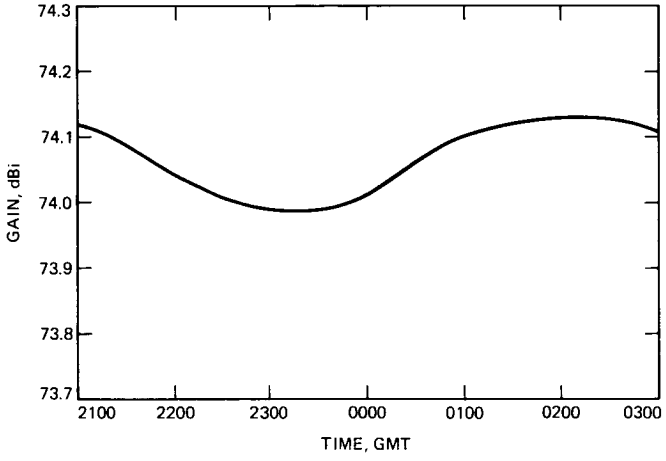

Fig. 2. Gain vs time with subreflector *y* and *z* focusing

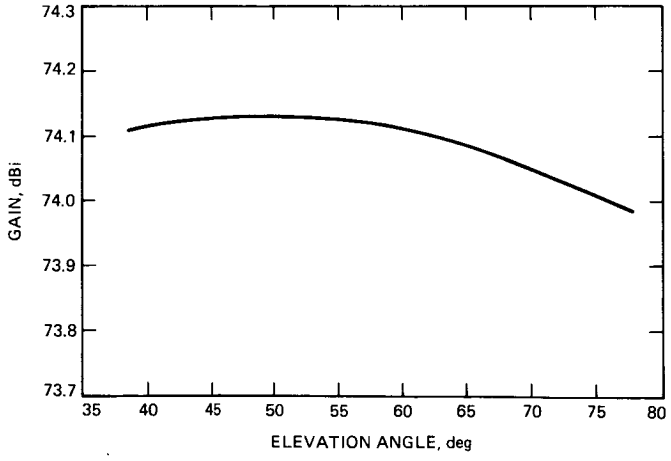

Fig. 3. Gain vs elevation angle with subreflector *y* and *z* focusing

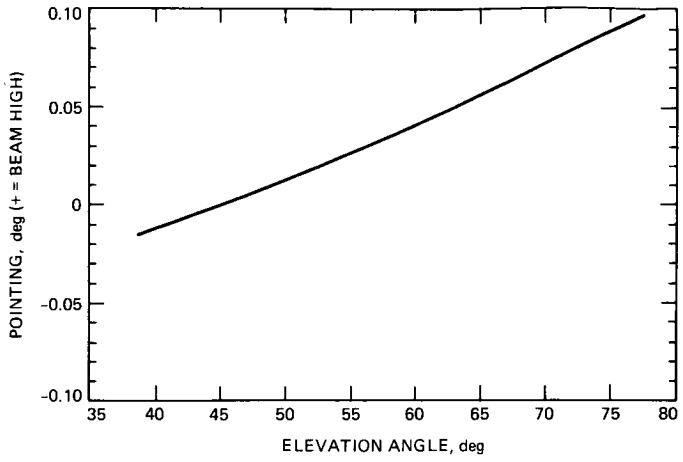

Fig. 4. Beam pointing vs elevation angle with subreflector *y* and *z* focusing

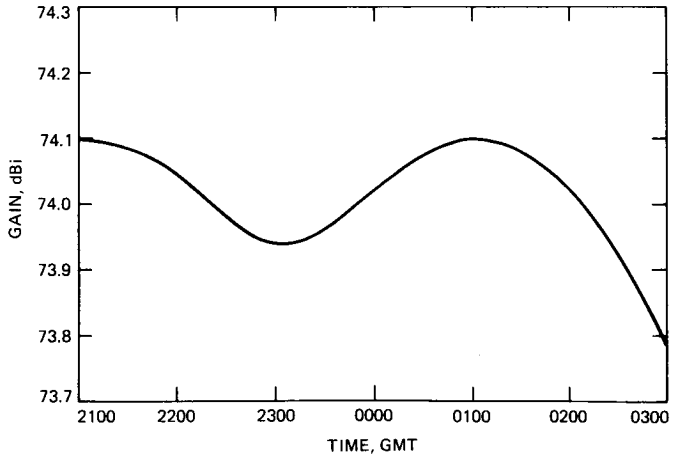

Fig. 5. Gain vs time with subreflector fixed at 64-degree elevation angle position

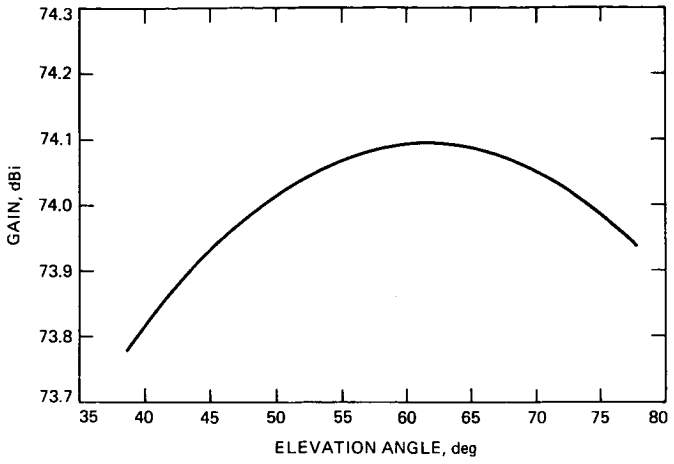

Fig. 6. Gain vs elevation angle with subreflector fixed at 64-degree elevation angle position

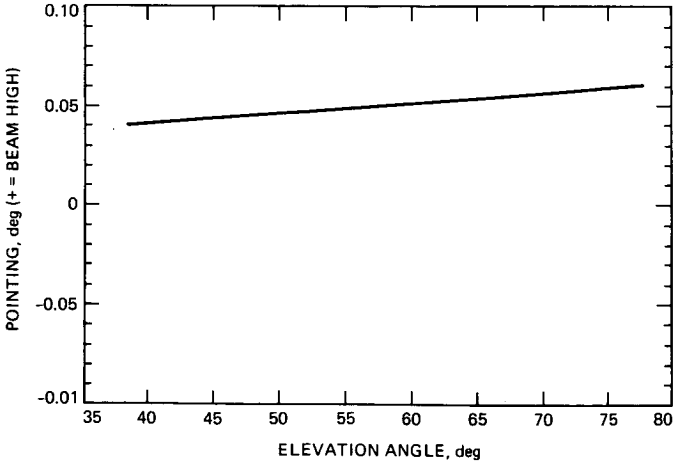

Fig. 7. Beam pointing vs elevation angle with subreflector fixed at 64-degree elevation angle position

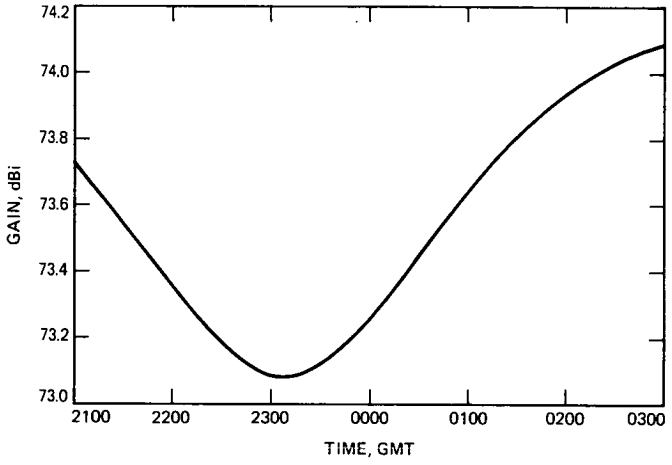

Fig. 8. Gain vs time with subreflector fixed at 34-degree elevation angle position

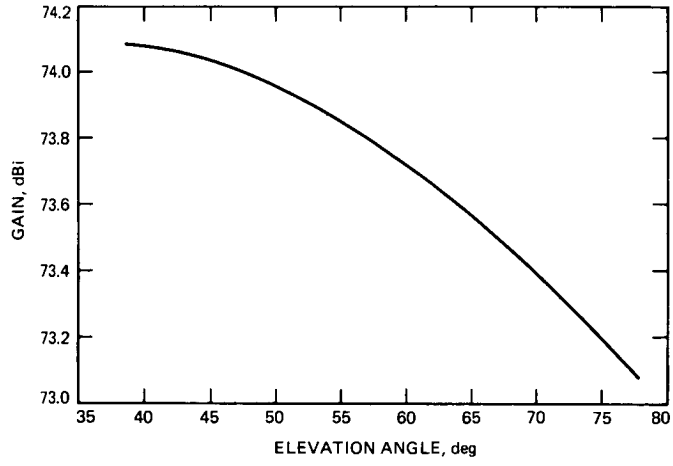

Fig. 9. Gain vs elevation with subreflector fixed at 34-degree elevation angle position

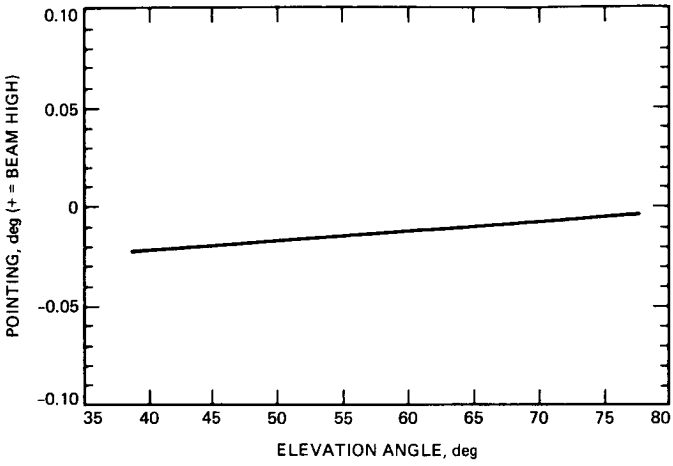

Fig. 10. Beam pointing vs elevation angle with subreflector fixed at 34-degree elevation angle position

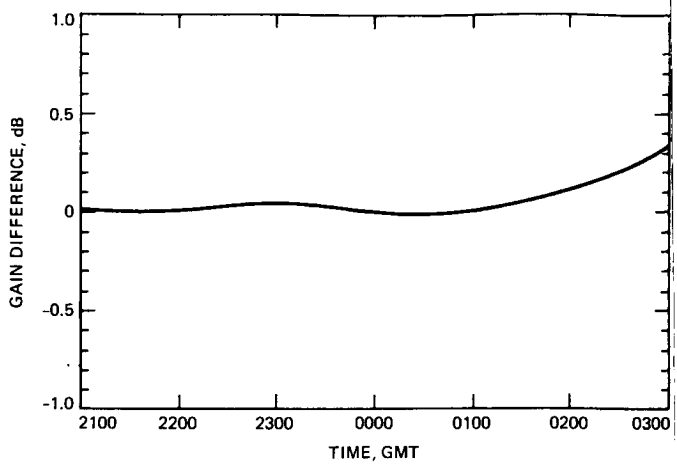

Fig. 12. Gain advantage of subreflector *y-z* focusing during encounter compared to subreflector fixed at 64-degree position

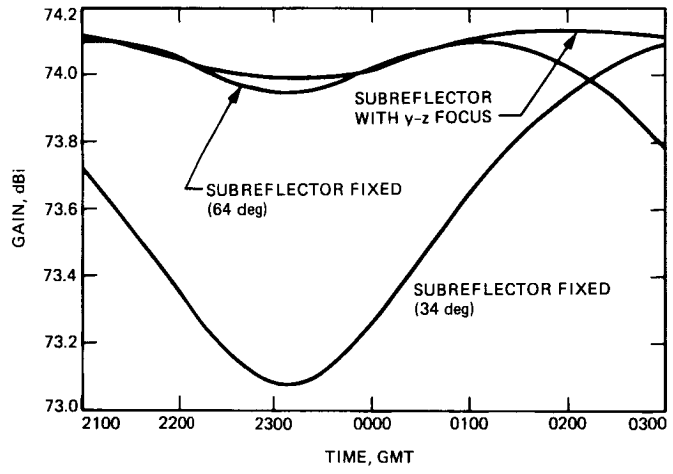

Fig. 11. DSS 43 antenna gain curves for different subreflector conditions, assuming perfect antenna pointing

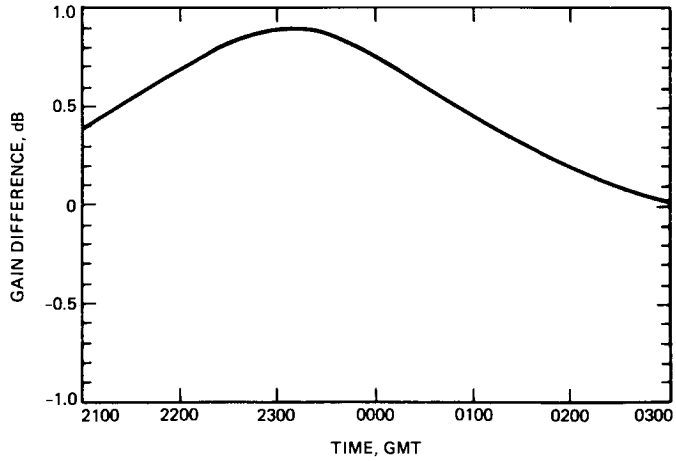

Fig. 13. Gain advantage of subreflector *y-z* focusing during encounter compared to subreflector fixed at 34-degree position

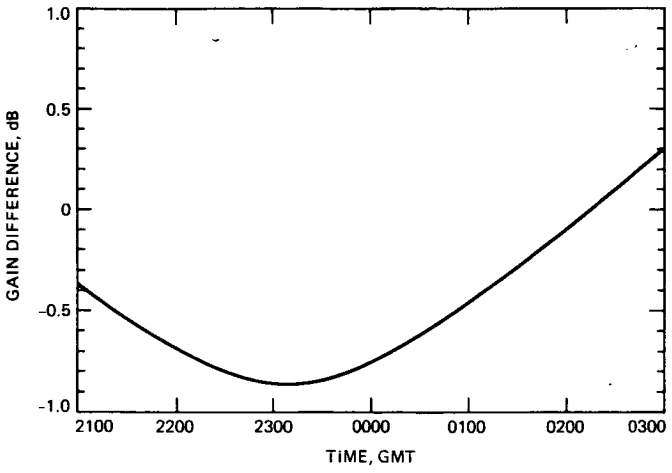

Fig. 14. Gain loss during encounter compared to 2-weeks previous performance, assuming perfect pointing ("−" equals loss)

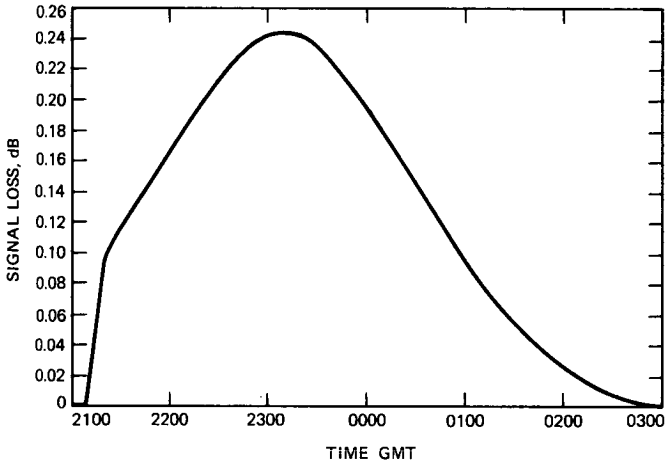

Fig. 16. Signal loss during encounter due to incorrect squint correction

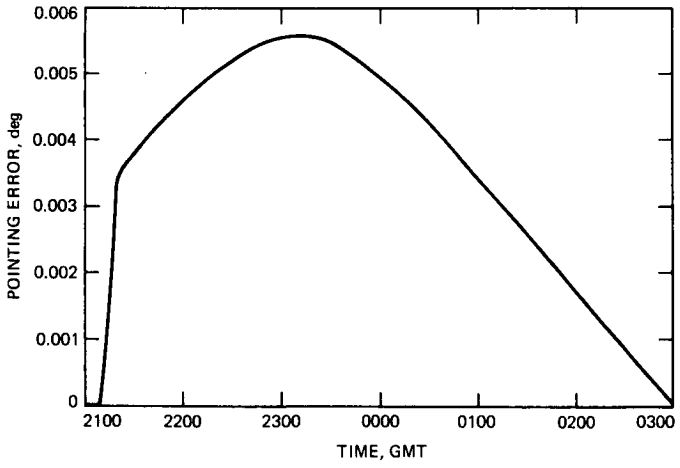

Fig. 15. Pointing error during encounter due to incorrect squint correction

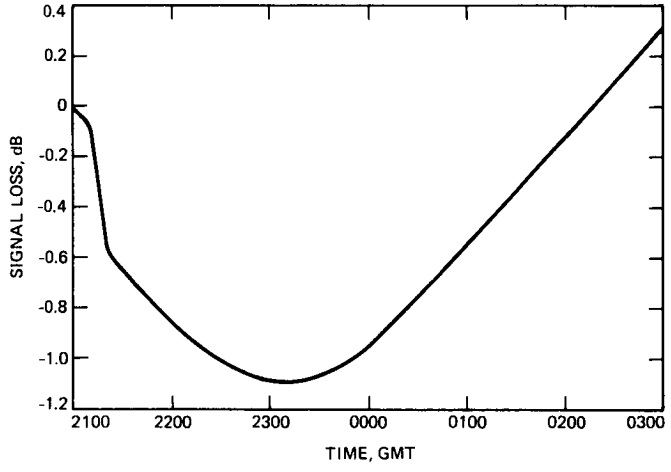

Fig. 17. Signal loss during encounter compared to earlier performance, due to both antenna gain loss and pointing error ("−" equals loss)